A Study on the Heat Transfer Performance of Evaporators Through Metal Foam of Wickless Loop Heat Pipe

Yong-Gy Chae, Hyun-Woo Won, Dong-Hyun Cho*

Department of Mechanical Engineering, Daejin University, Korea
Email: chodh@daejin.ac.kr

The fluid that operates in wickless loop heat pipes boils and condenses as an outcome of tiny temperature variations, transferring a significant quantity of heat flux. An insulating unit, a condenser, and an evaporator make up a metal wickless loop heat pipe. A heating of the evaporator in the lower section of the wickless loop heat pipe evaporates the fluid which is used within the metal foam evaporator units and the evaporated steam ascends to the condenser in the top section to produce heat in the reaction of the cooling fluid within the tube. A research study was carried out using R134a refrigerant as the fluid of operation of a wickless loop heat pipe to observe shifts in boiling thermal transfer shows in response to shifts in the refrigerant temperatures, mass flows, and the temperature of the oil used for heating an evaporator with metal form. A current study's findings indicate that there are significant patterns in the wall heat flux of the evaporators with metal foam. This is important for predicting the exact location of gas generation and gas fractions in an evaporator with metal form. Natural convection was thought to cause the oil flow near the metal foam evaporating tube. The wickless loop heat pipe's rate of boiling producing steam rose in tandem with the oil temperatures in the evaporator with metal foam. Compared to low-density metal foam, higher-density metal foam has a greater heat transmission rate.

Keywords: Wickless Loop Heat Pipe, Evaporator, Metal form, Performance.

1. INTRODUCTION

Wickless loop heat pipe systems for cooling can increase the effectiveness of cooling because they utilize the unused energy from the operating fluid's boiling and condensation to release heat, allowing for the implementation of high-performance systems at lower costs, smaller sizes, and lower power consumption(1,2). Therefore, wickless loop heat pipe cooling systems with high-speed shaft rotation can be produced for a lot less money than other cooling systems since they don't need components like chillers and pumps for circulating cooling fluid[(3)]. Chen[(4)] discovered that an excursive unstable event could be distinguished from static stability and that boiling channels contained regions where pressure drops

increased as flow velocity dropped. Knaani (5) built a cooling system for electronic components utilizing a wickless loop heat pipe and studied the rise and fall of refrigerant pressure at different stages of the cycle both experimentally and theoretically. Two parallel vertical tubes were put in a natural circulation loop, and Lee et al. (6) investigated the uncertainty brought on by nucleation in static variability. The results of the investigation showed that when slug bubbles formed in the channel, a novel geysering phenomenon happened.

In the current work, modeling techniques were used to assess the efficiency of heat transfer, and the findings were cross-checked with data from experiments. Simulations focused on the heat allocation effectiveness of the evaporator with the help of the wickless loop heat pipe, which may release the substantial quantities of heat produced by the rapid variation of the high-speed variation shafts of high voltage engines, generators, and huge turning lathes.

2. EXPERIMENTAL APPARATUS AND METHOD

2.1 Experimental Apparatus of the Wick Loop Heat Pipe

The setup that was used to evaluate the wickless loop heat pipe's heat transfer performance is presented in Figure 1. A wickless loop heat pipe is equipped with a separate boiling segment called the evaporator and a cooling section called the condenser. The wickless loop heat pipe's evaporator and condenser were complexes of pipes made up of numerous pipes and were built in order for pipes collected at the top and bottom to connect them to one another. The wickless loop heat pipe's evaporator and condenser are linked to one another by conveying pipes that control working fluid flows, and the condenser is equipped with an emissions valve and a gas/liquid separation to collect non-condensable gases. Because of these features, the condenser in a wickless loop heat pipe must always be located higher than the evaporator in order to create a sufficient pressure differential for the fluid that is being used to circulate.

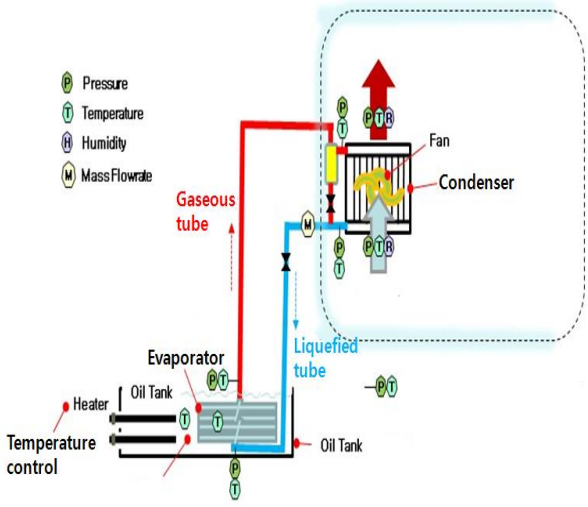

Fig. 1 Experimental setup to test heat transference implementation of the wickless loop heat pipe

A wickless loop heat pipe research facility's schematic diagram is shown in Figure 2. The dimensions of the condenser are 700 mm in height, 1100 mm in length, and 500 mm in width. On a condenser, 8015 mm in thickness and 1,100 mm in dimension of copper pipes were fitted. Moreover, exhaust ports were installed on the condenser to allow for the filling of working fluid and the exhausting of non-condensable gases. As depicted in Fig. 2. The height variance of the condenser and the evaporator was fixed to 1.7 meters for the 7kW grade wickless loop heat pipe performance trials. The conveying pipe that joins the condenser and evaporator has an outer diameter of 25 mm. The conveying zone associated with the evaporator and condenser was inspected with high-pressure nitrogen to ensure there were no leaks, and it was sealed with 50mm thick glass fibers to minimize the losses of heat to the exterior of pipes that happen if the working fluid passes in the flow of water and steam pipes. The evaporator's working fluid intake and outflow were equipped with Pressure Transducers (P21AA, 0~2MPa) to measure the individual data gathered at the performance experimental facility. This makes it possible to monitor and compare the vapor pressure of the working fluid with the temperature. At the inlet/outlet of the condensation and the evaporator itself, a single thermocouple (K-type sheath dirt, 1.6mm OD) is fitted. Three thermocouples were fitted at the inlet and outlet, correspondingly, to determine the oil heat in the evaporator housing and the air temperature in a condenser. A hybrid recorder (64 channels) was utilized to collect and save the results of the experiment. A condensate refrigerant flow rate was measured by installing a refrigerant flowmeter at the condenser outlet tube. The beginning temperatures in wickless loop heat pipe performance trials are critical. As a result, the non-condensable gases that were still inside the tube were released, preserving a steady level of vacuum in typical conditions. We used R-134a as our operating fluid. A scale was utilized to determine the amount of fluid that was delivered. When the study was run, a slider thermostat was placed to keep the oil heat in the oil housing, which provides heat to the evaporator, between 20 and 80 degrees Celsius. At each layer, the heat of the working fluid at the condenser, evaporator, and outflow were evaluated.

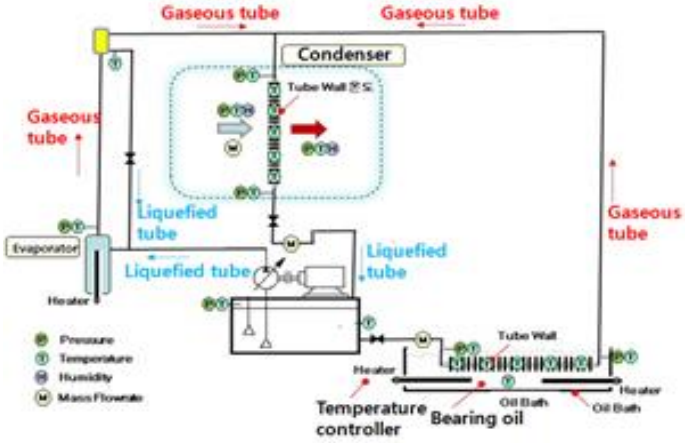

Fig. 2 Diagrammatic representation of the wickless loop heat pipe experimental setup

Figure 3 shows a schematic diagram of metal foam. Fig. 4 shows an evaporating tube with metal foam. The metal foam thickness is 4, 6, and 8mm.

The evaporator's schematic diagram in metal form is shown in Figure 5. The evaporator with metal foam is shown in Figure 6. An evaporator with metal foam of a two-phase thermosyphon of loop type is shown in Figure 7. For the purposes of this investigation, a 6.5kW grade loop-type thermosyphon heat exchanger with a metal evaporator measuring 699mm in diameter outside, 630mm inside, and 150mm tall was used. Furthermore, 98 copper pipes with a diameter of 12 mm were inserted inside the evaporator using metal forms, and 100 copper pipes with the same diameter were put in outside the evaporator.

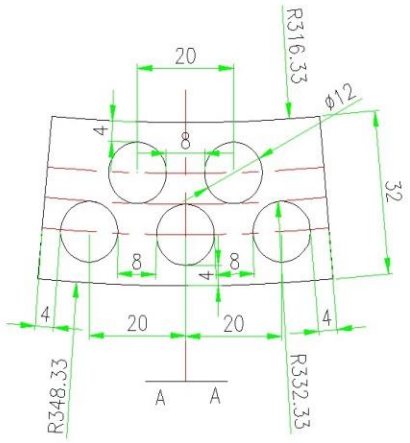

(a) Metal foam thicknenss 4mm

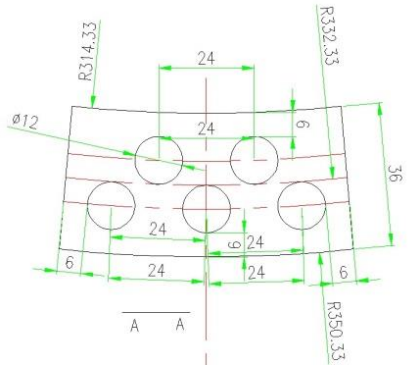

(b) Metal foam thicknenss 6mm

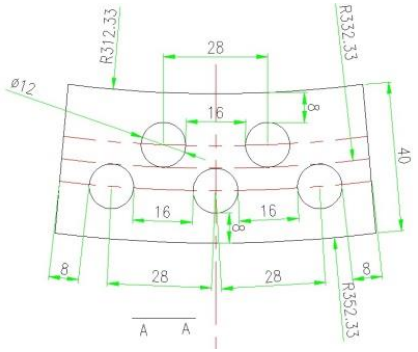

(c) Metal foam thicknenss 8mm

Figure 3: Schematic diagram of metal foam

Figure 4: Evaporating tube with metal foam

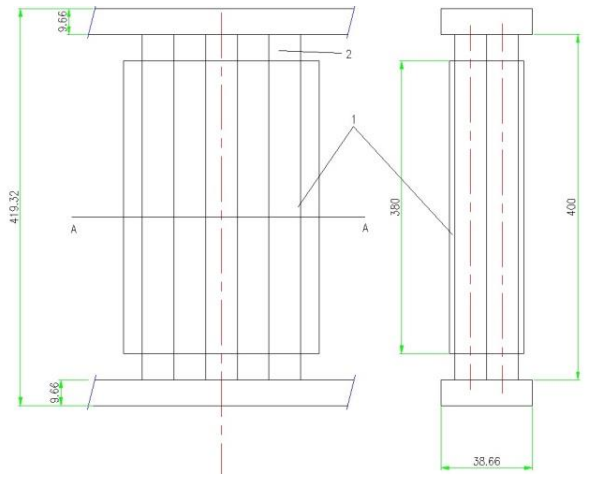

Figure 5: Schematic diagram of the evaporator with metal foam

Figure 6: Evaporator with meatl foam of the wickless loop heat pipe

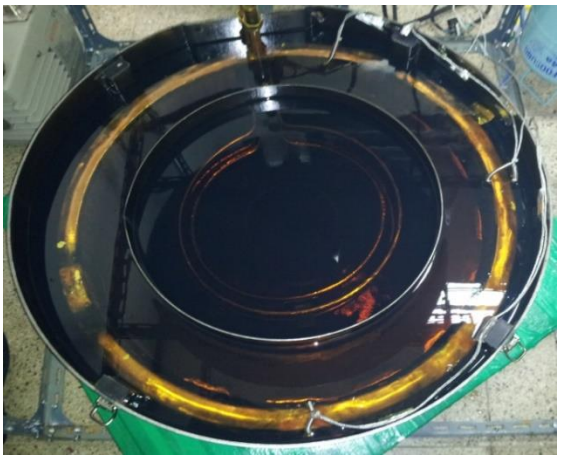

Fig. 7: Evaporator with meatl foam of wickless loop heat pipe

3. RESULTS

3.1 Phase Change Model Simulation of the Evaporator with Metal foam of the Wickless Heat Pipe

Fig. 8 shows a schematic diagram of the evaporating tube with metal foam. The form of an early simulation for an evaporator using metal foam phase transformation models and associated boundary conditions is depicted in Figures 9 through 11. The RPI (Rensselaer Polytechnic Institute) simulation with the nucleation, development, and separation of bubbles on walls supplied by ANSYS FLUENT v13 were used in a preliminary simulation. The model shape and borderline conditions were also set using the same ANSYS FLUENT v13 boundary settings.

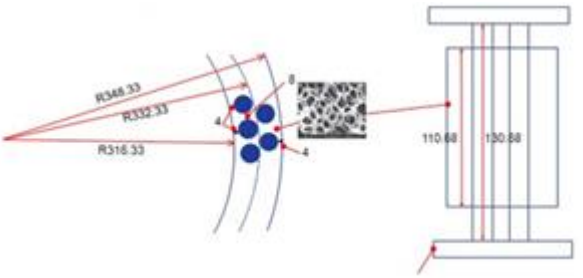

Fig. 8: Schematic diagram of the evaporating tube with metal foam of wickless loop heat pipe

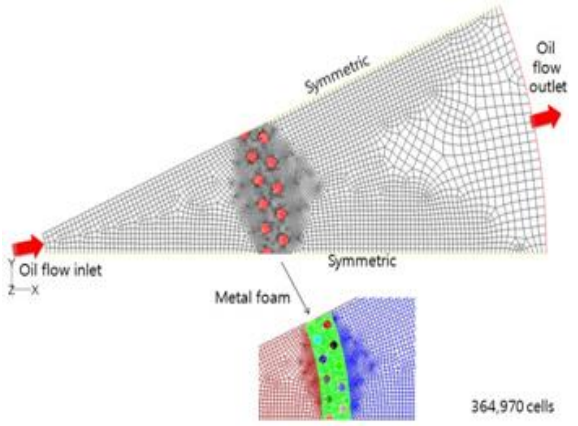

Fig. 9: The modeling of the evaporating tube with metal foam

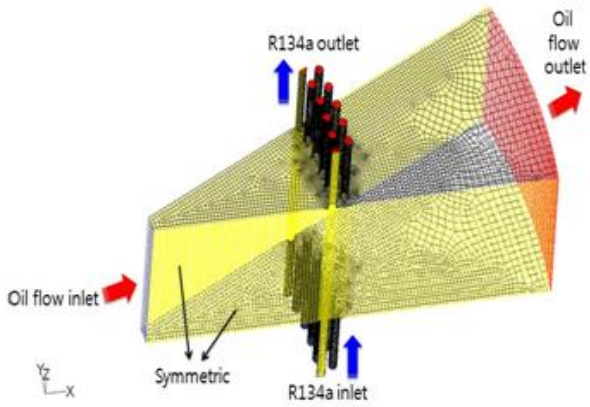

Fig. 10: The grid generation of evaporating tube with metal foam

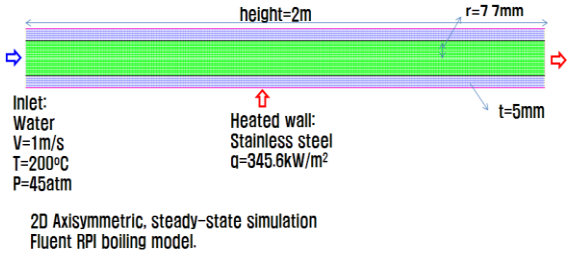

Fig. 11: The form of the initial simulation and associated boundary conditions for phase transition simulations in evaporators

The gas fraction, gas rate, liquid velocity, and liquid distributions of heat in the oil enclosures of the evaporator with metal foam of the wickless loop heat pipe are displayed in Figure 12. A velocity distribution obtained from the simulation aimed at forecasting oil flows in the evaporator equipped with metal foam suggested that an impact of oil flows arising from the variation of the shaft on the oil flows near the heat pipe ought to be minimal. The oil flows near the evaporating tube with metal foam are assumed to be convection from

nature based on the results of the simulations that were used to estimate the oil flows in the evaporator oil housing.

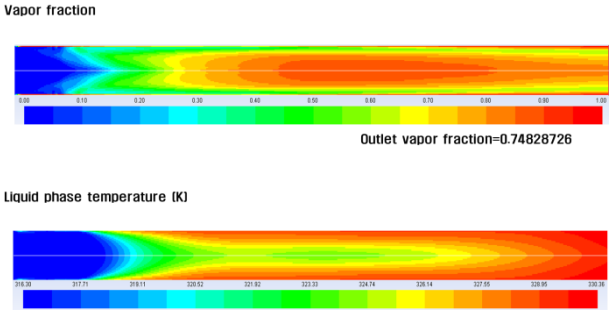

Fig. 12: Gas percentage, gas velocity, liquid temperature, and liquid velocity ratios

Fig. 13 and Fig. 14 show an analytical model considering the evaporator with the metal foam. The thermal resistance is measured in parallel by conduction heat transfer and convective heat transfer. Table 1 shows the simulation case. Fig. 13 and Fig. 14 show the distributions of vapor volume fraction, and wall temperatures in the evaporating tube with metal foam. It can be seen that in the evaporating tube with metal foam, the gas starts to gradually emerge from the wall and join in the middle; this outcome was in line with the pattern of gas velocity. Furthermore, based on wall heat flux, there were strong trends for predicting the location of gas generation and gas fractions in an evaporating tube with metal foam. As porosity decreased, vapor fraction increased.

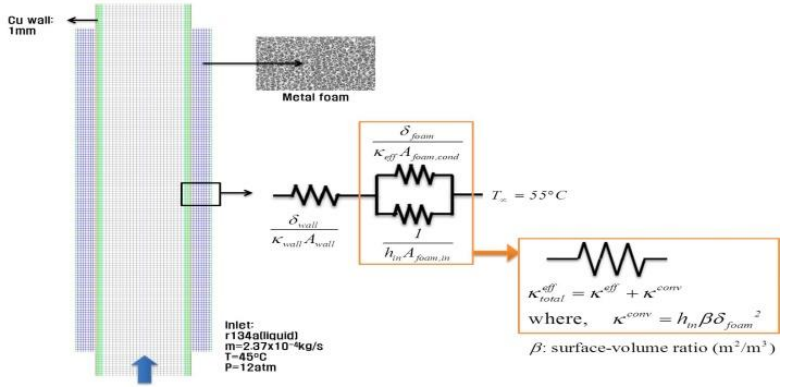

Fig. 13 Analytical model considering the metal foam evaporator of the wickless loop heat pipe

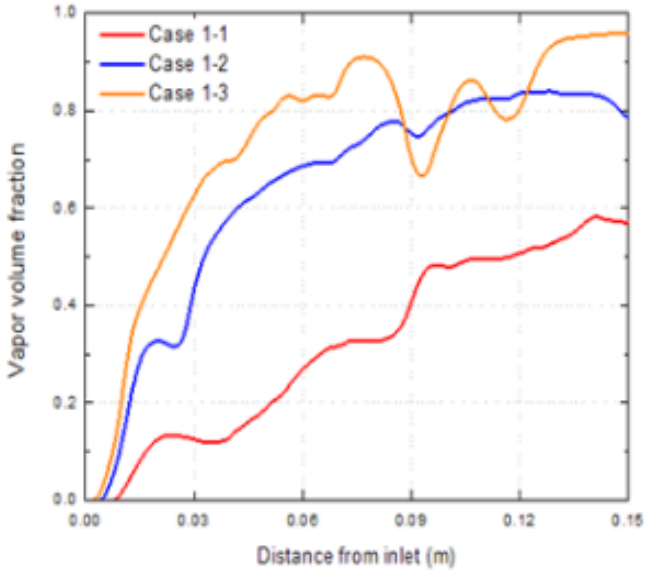

Fig. 13 Vapor volume fraction vs. distance from inlet

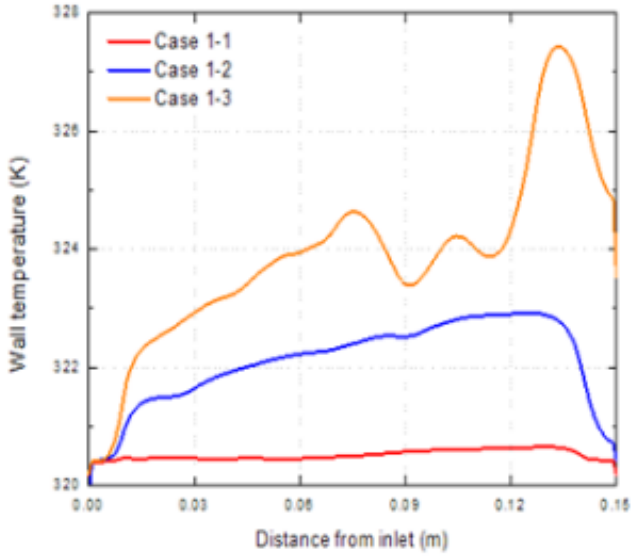

Fig. 14: Wall temperature vs. distance from inlet

Table 1: Simulation case.

case		d_f (m)	d_p (m)	ε	δ_{foam} (m)
1	1	$0.5x10^{-3}$ (assumed)	$4x10^{-3}$	0.9225	$4x10^{-3}$
	2		$3x10^{-3}$	0.8157	
	3		$2x10^{-3}$	0.5770	

3.2 Results of Experiments for Evaporator with Metal foam of the Wickless Loop Heat Pipe

Figure 15 to Figure 17 show the results of experiments for evaporator with metal foam and Figure 15 displays alterations in the oil temperature of the evaporator allowing to heat input of oil. 134a is the refrigerant that was utilized in the trials. Six to nine kg of refrigerant were charged per hour during the studies. As the oil temperature in the evaporator with metal foam increased, heat flux of evaporator increased. Therefore as the oil temperature the pace at which the wickless loop heat pipe produced boiling steam rose in the evaporator with metal foam.

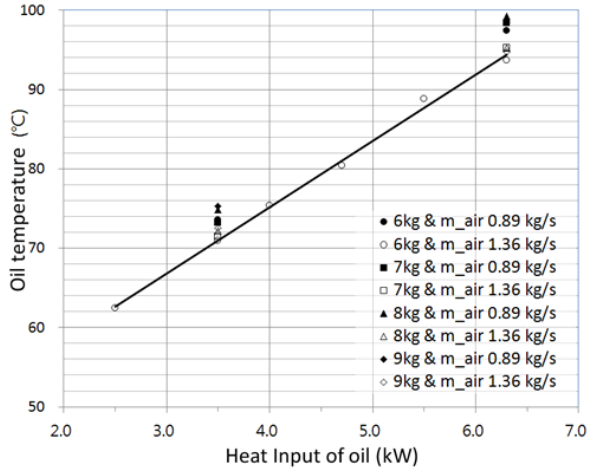

Fig. 15: Oil temperature of evaporator with metal foam of the wickless loop heat pipe according to heat input of oil

Figure 16 shows oil temperature of evaporator with low density and high density metal foam. 134a is the refrigerant that was utilized in the trials. The studies were carried out using refrigerant charge rates ranging from 6 to 9 kg and condenser air flow rates between 0.58 and 1.36 kg/s. As the oil temperature in the evaporator with metal foam increased, heat flux of evaporator improved. Compared to low density metal foam, high density metal foam has a greater heat transmission rate. Figure 17 shows temperature difference of ambient temperature and oil temperature according to ambient temperature changes. 134a is the refrigerant that was utilized in the trials. Heat transfer performance in accordance with the increased oil temperature increases.

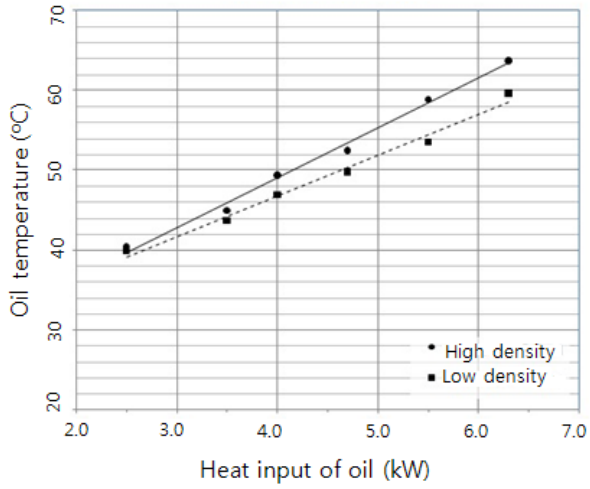

Fig. 16: Oil temperature of evaporator with low density and high density metal foam according to heat input of oil

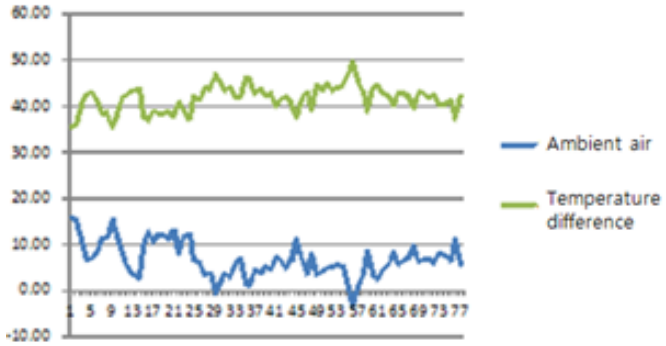

Fig. 17: Temperature difference of ambient temperature and oil temperature according to ambient temperature changes

4. CONCLUSIONS

R-134a was utilized as the working fluid in research of the evaporators with metal foam of wickless loop heat pipe for heat release from rapidly rotating shafts. The experimental findings contrasted with the simulation findings regarding variations in evaporator temperatures among oil and evaporator temperatures based on condenser cooling airflow ratios. The following is a summary of the findings:

(1) Based on the internal heat flux of the evaporator units with metal foam, significant patterns for predicting the position of gas generation and gas fractions in an evaporating tube were revealed.

(2) Convection from the air was thought to cause the oil flow near the metal's foam evaporating tube.

(3) The wickless loop heat pipe's rate of boiling producing steam rose in tandem with the oil temperatures in the evaporator with metallic foam.

(4) Compared to low-thickness metal foam, high-density metal foam has a greater heat transmission rate.
(5) Heat transfer performance in accordance with the increased oil temperature increases.

NOMENCLATURE

dp :Pore diameter(m)
d_f :Fiber diameter(m)
δfoam :Thickness of foam
ε : Porosity

References

[1] Lee, K.W., Chang, K.C., Lee, K.J., Lee, Y.S.and Hong, S.H., 1995, Heat Transportation Technology Separate Heat Pipe Heat Exchanger, Energy R&D Technical Analysis Report, Vol.17, No.1&2, pp.154~166

[2] Kyuil Han, Dong-Hyun Cho and Tae-Woo Lim. 2005, Characteristics of Boiling Heat Transfer of Thermosyphon HeatExchangers with Helical Grooves

[3] C. Tarau, M. T. Ababneh, W. G. Anderson, A. R. Alverez-Hernandez, J. T. Farmer and R. Hawkins, "Advanced Passive Thermal eXperioment (APTx) for Warm-Reservoir Hybrid-Wick Variable Conductance Heat Pipes on the International Space Station (ISS)," in 48th International Conference on EnvironmentalSystem (ICES), 2018.

[4] B.S. Taft, F.F. Laun, S.M. Smith, D.W. Hengeveld, Microgravity Performance of a Structurally Embedded Oscillating Heat Pipe, Journal of Thermophysics and Heat Transfer. 29 (2015) 329–337. https://doi.org/10.2514/1.T4151.

[5] B.L. Drolen, C.D. Smoot, Performance Limits of Oscillating Heat Pipes: Theory and Validation, Journal of Thermophysics and Heat Transfer. 31 (2017) 920–936. https://doi.org/10.2514/1.T5105.

[6] B.S. Taft, S.M. Smith, ASETS-II Oscillating Heat Pipe Space Flight Experiment: Ground Truth Results, in: American Society of Mechanical Engineers Digital Collection, 2017. https://doi.org/10.1115/HT2017-4706.

[7] B.L. Drolen, C.A. Wilson, B.S. Taft, J. Allison, K.W. Irick, Advanced Structurally Embedded Thermal Spreader Oscillating Heat Pipe Micro- Gravity Flight Experiment, Journal of Thermophysics and Heat Transfer. 36 (2022) 314–327. https://doi.org/10.2514/1.T6363.

[8] T. Yan, Y. Zhao, J. Liang, F. Liu, Investigation on optimal working fluid inventory of a cryogenic loop heat pipe. International Journal of Heat and Mass Transfer, 2013. 66: p. 334-337.

[9] C. Du, L. Bai, G. Lin, H. Zhang, J. Miao, D. Wen, Determination of charged pressure of working fluid and its effect on the operation of a miniature CLHP. International Journal of Heat and Mass Transfer, 2013. 63: p. 454-462.

[10] T. Yokouchi, X. Chang, K. Odagiri, H. Ogawa, H. Nagano and H. Nagai, Supercritical Startup Experiment of Cryogenic Loop Heat Pipe for Deep Space Mission. in 51st International Conference on Environmental Systems. 2022. Saint Paul, USA.

[11] L. Bai, L. Zhang, G. Lin, J. He and D. Wen, Development of cryogenic loop heat pipes: A review and comparative analysis. Applied Thermal Engineering, 2015. 89: p. 180-191.

[12] L. Bai, G. Lin, H. Zhang, J. Miao and D. Wen Experimental study of a nitrogen-charged cryogenic loop heat pipe. Cryogenics, 2012. 52: p. 557-563.

[13] Y. Guo, G. Lin, H. Zhang, and J. Miao, Investigation on thermal behaviours of a methane charged cryogenic loop heat pipe. Energy, 2018. 157: p. 516-525.